A Feasibility Study towards Ultra-Thin PV Solar Cell Devices by MOCVD Based on a p-i-n Structure Incorporating Pyrite

A.J. Clayton[a]*, S.J.C. Irvine[a], V. Barrioz[a], G. Zoppi[b], I Forbes[b] and W.S.M. Brooks[a]
[a]CSER, Glyndŵr University, OpTIC Glyndŵr, St Asaph Business Park, LL17 0JD
[b]NPAC, Northumbria University, Ellison Building, Newcastle upon Tyne, NE1 8ST
*andy.clayton@optictechnium.com / 01745 535 213

Abstract

FeS_x layers were deposited onto aluminosilicate glass substrates over a temperature range of 180°C to 500°C using a horizontal AP-MOCVD reactor. $Fe(CO)_5$ was used as the Fe source in combination with t-Bu_2S_2 or t-BuSH as S precursor to control the rate of reaction and film stoichiometry. The Fe and S partial pressures were kept at 7.5 x 10^3 and 3.0 mbar, giving a gas phase S/Fe ratio of 400. Reactions followed a non-Arrhenius relationship at higher temperatures. XRD revealed mixed FeS_x phases in the layers, which consisted mainly of FeS and $Fe_{1-x}S$. Post growth annealing of the FeS_x films using S powder in a static argon atmosphere and temperatures ranging from 250°C to 400°C was carried out using a 30 minute soak time. Characterisation by XRD confirmed a transitional phase change to FeS_2 for the S anneal at 400°C. These films were highly absorbing in the visible region of the solar spectrum, which extended into the NIR. Devices with a p-i-n structure were produced using either a sulphurised or non-sulphurised FeS_x *i*-layer, and compared to p-n devices without an *i*-layer. A non-sulphurised p-i-n device had the best *I-V* results, which was attributed to reduced lateral inhomogeneity across the device relative to the thinner p-n device structures. Devices with sulphurised FeS_x *i*-layers performed least efficiently which is suspected to be due to a less defined FeS_x/CdS junction caused by severe conditions during the S annealing process.

Introduction

Pyrite (FeS_2) has been investigated over the last couple of decades due to its high absorption coefficient, which is in the order of 10^5 cm^{-1} in the visible region of the solar spectrum. The direct band gap of 0.95 eV reported by Ennaoui and co-workers [1] has been accepted by most researchers. This makes it a desirable material for photovoltaic (PV) applications where it may be possible to increase photon capture at longer wavelengths than conventional thin film PV cells, such as CdTe, towards the near infrared (NIR) region.

Pyrite has been deposited by metal organic chemical vapour deposition (MOCVD) using several different reactor configurations. Schleigh and Chang [2] carried out MOCVD of pyrite in a hot walled horizontal reactor at reduced pressure (LP) using iron pentacarbonyl ($Fe(CO)_5$) with various S precursors, including hydrogen sulphide (H_2S), *tert*-butylsulphide (t-BuS) as well as ditertiarybutyl disulphide (t-Bu_2S_2). They reported that stoichiometric FeS_2 was only possible when t-Bu_2S_2 was used as the S source with growth temperatures of 480°C or higher being employed. Difficulty in obtaining stoichiometric FeS_2 is due to the large difference between the vapour pressures of the Fe and S precursors. Large partial pressures of S have to be employed to compensate for its low vapour pressure relative to $Fe(CO)_5$. Therefore high S/Fe ratios are necessary for the MOCVD process to grow stoichiometric FeS_2 [2-4].

Höpfner *et al*. [4] found pyrrhotite phases ($Fe_{1-x}S$) to be present in the majority of layers. At temperatures below 450°C the layers consisted mainly of marcasite (FeS_2), with the pyrite fraction increasing with growth temperature replacing marcasite until pure pyrite was obtained at 525°C.

Pyrite can also be prepared by sulphurising Fe or FeS films. Ferrer and co-workers [5] carried out sulphurisation of Fe films using S powder in glass ampoules at temperatures between 252°C (325K) and 502°C (725K) with soak times ranging from zero to 20 hours. They reported all films to be pyrite after 20 hour soak times confirmed by X-ray diffraction (XRD) characterisation.

Zheng *et al*. [6] obtained single phase pyrite annealing FeS layers in a S atmosphere for 10 hours. This group observed a transitional phase to pyrite and marcasite at 400°C. Raising the temperature to 500°C led to single phase pyrite. The pyrite XRD peak intensities were observed to reduce when the

sulphurisation temperature was raised to 600°C.

Application of pyrite thin films has had limited success in PV devices and has not really improved since Ennaoui and co-workers [7] reported an efficiency (η) of around 2.8 % at AM1.5. There are issues with pyrite films such as low photovoltages [8] which could be related to S deficiency in the layer. Characterisation of Co-doped pyrite films with variable carrier concentration by Ellmer and Tributsch [8] highlighted possible Fermi level pinning at the surface, suggesting a high density of defects.

This paper discusses a feasibility study towards using pyrite as an ultra-thin *i*-layer, incorporating it into a CdTe-based device structure developed by Barrioz *et al.* [9] to investigate whether absorption in the device can be enhanced. FeS_x layers have been deposited by MOCVD at atmospheric pressure (AP), which is more suitable for scale up. Devices have been produced by depositing FeS_x layers onto CdS, which were then sulphurised in an argon atmosphere and capped with a p^+ CdTe:As layer. Gold back contacts were used to complete the device and initial results of device performance is reported.

Experimental

AP-MOCVD was used to deposit FeS_x on to aluminosilicate glass using a horizontal quartz reactor tube. $Fe(CO)_5$ was used in combination with t-Bu_2S_2 or tertiarybutyl thiol (t-BuSH) to control the rate of reaction and the film stoichiometry. The quartz reactor chamber was heated by a 1kW infrared heater using a thermocouple inserted into a groove under the graphite susceptor for temperature control. Temperatures employed ranged from 180°C to 500°C.

Precursor partial pressures were controlled to give S/Fe ratios of 400 for the majority of experiments. Step measurements using atomic force microscopy (AFM) was carried out on the FeS_x layers after experiments to obtain the thickness for each film.

Results and Discussion

The reactor configuration suffered from premature reaction of the $Fe(CO)_5$ at temperatures >400°C. Therefore, reactions at the substrate followed a non-Arrhenius relationship at higher temperatures. This is typical of a horizontal AP-MOCVD process. The deposition rate on the substrate at the higher temperatures where single pyrite is favoured was extremely slow due to the parasitic growth inside the injector and at the reactor walls. The reactor configuration was therefore more suited to low temperature deposition. This resulted in mixed phases in the layers, which were predominantly troilite (FeS) and pyrrhotite ($Fe_{1-x}S$) as determined by XRD. *Fig. 1* represents typical 2θ positions from FeS_x films grown by MOCVD at low temperature.

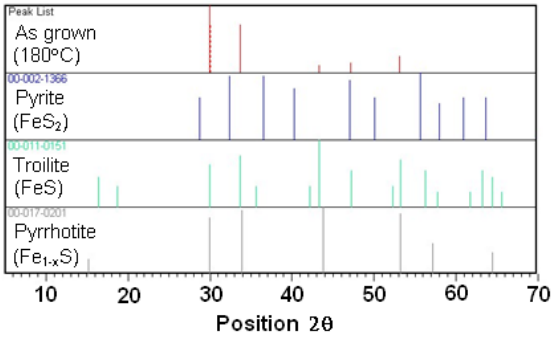

Fig. 1: XRD peaks from an as-grown film deposited at 180°C using t-BuSH as S precursor.

The S deficient MOCVD FeS_x films were sulphurised using S powder in an enclosed graphite chamber with an argon atmosphere and heated to temperatures between 250°C and 400°C. Soak times of 30 minutes were used and the films were then characterised by XRD. The FeS_x film sulphurised at 400°C revealed a conversion to marcasite and pyrite whilst retaining some of the troilite (FeS). *Fig. 2* shows the XRD peaks of the same film represented in *Fig. 1*, but after S annealing, and clearly shows a peak transition in the 2θ positions.

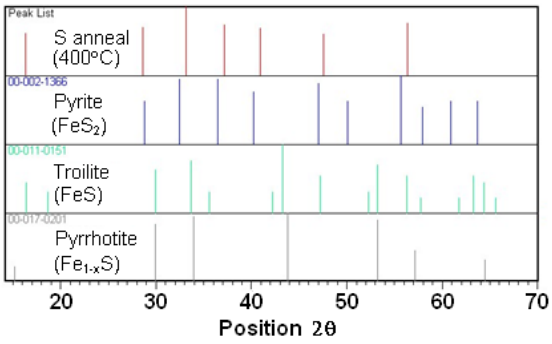

Fig. 2: XRD peaks from a FeS_x film sulphurised at 400°C for 30 minutes.

It was deduced that higher sulphurisation temperatures and longer annealing times would be required to achieve single phase pyrite as reported [5, 6, 10]. Comparison of

transmittance (T%) spectra of non-sulphurised and sulphurised films showed an increase in absorption in the visible region of the solar spectrum after S annealing. *Fig. 3* shows T% spectra for the film represented in *Figs. 2* and *3* before and after S annealing.

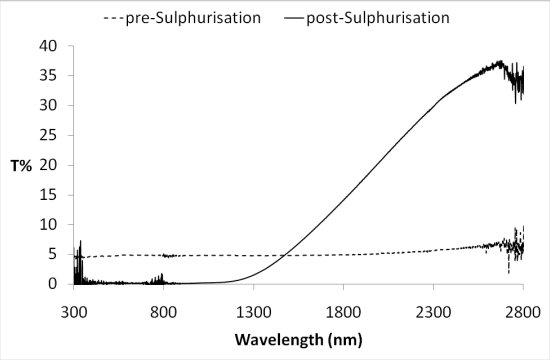

Fig. 3: Comparison of Transmittance spectra of a film pre- and post-sulphurisation.

Absorption in the visible region and towards the near infrared (NIR) can be observed to increase such that T% through the film is close to zero. This occurs even for a FeS_x layer consisting of only a fraction of pyrite. The absorption coefficient, α, was calculated using the data collected from the T% spectra for the S annealed film, which had values from 1.2 x 10^5 cm^{-1} at 1400 nm to 2.6 x 10^5 cm^{-1} at 400 nm. This shows that α reaches expected values for single phase pyrite even when it exists with other Fe-S phases in the layer.

A similar change in the visible region in the T% spectrum for FeS_x layers on CdS deposited using t-BuSH before and after S annealing was observed. The T% spectrum for the FeS_x layer on CdS deposited using t-Bu_2S_2 as S precursor showed little change between the non-sulphurised and sulphurised film.

Devices with a p-i-n structure were produced using a 250 nm CdTe:As p^+ layer and a 240 nm CdS n-type layer on ITO coated aluminosilicate glass substrates. Sandwiched between these were *i*-layers, which were either sulphurised or non-sulphurised FeS_x. For control, devices without an *i*-layer were also tested. Mean results from *I-V* measurements from 6-8 contacts, depending on the device, for selected samples that gave best efficiencies (η) are displayed in *Table 1*.

The thickness of the sulphurised FeS_x layers has been assumed to be the same thickness as the equivalent non-sulphurised layers. Reports [5, 10] on measured thicknesses of films before and after S annealing noted that the layer thickness increased with S annealing. However, the S annealing experiments reported in the literature were carried out for many hours, whereas S annealing experiments carried out in this research had 30 minute soak times.

Sample	Jsc (mA/cm^2)	Voc (mV)	η %	FF %	FeS_x (nm)
t-BuSH (no S anneal)	10.77	498.33	2.82	52.25	99.50
Std. Dev.	0.68	10.33	0.38	4.08	30.41
t-BuSH (S anneal)	6.26	221.84	0.60	31.90	99.50
Std. Dev.	1.87	113.38	0.36	15.75	30.41
t-BuS_2S_2 (no S anneal)	8.38	318.13	1.46	39.89	53.50
Std. Dev.	3.00	179.47	0.92	18.56	123.74
t-Bu_2S_2 (S anneal)	3.12	179.80	0.20	32.38	53.50
Std. Dev.	1.91	60.51	0.19	3.79	123.74
p-n device 2	10.36	394.00	2.38	52.67	0.00
Std. Dev.	1.07	183.86	1.16	10.63	-
p-n device 1	10.63	251.29	1.02	28.89	0.00
Std. Dev.	2.54	168.96	0.84	14.66	-

Table 1: Averaged I-V results for p-i-n devices with sulphurised and non-sulphurised FeS_x i-layers, and for devices without a FeS_x i-layer.

The devices with FeS_x layers that had not been annealed in a S atmosphere performed much better than the devices with equivalent FeS_x layers that had been sulphurised. It is possible that the S annealing process was too harsh for the CdS/FeS_x junction, particularly as the FeS_x layer was less than 100 nm in thickness. The sulphurisation process may have affected the junction causing the CdS/FeS_x interface to be less defined from S diffusion between the two layers.

The standard deviation (σ) for J_{sc}, V_{oc} and η was large for the non-sulphurised p-i-n structure with FeS_x layer deposited using t-Bu_2S_2. This is likely to be due to the poor thickness uniformity across this device which is reflected in the high σ.

The best performing device with non-sulphurised FeS_x layer deposited using t-BuSH had the lowest σ for J_{sc}, V_{oc} and η. However, comparison of this device with the p-n devices without the FeS_x *i*-layer shows little difference in the calculated mean short circuit current (J_{sc}), even though σ is larger for the p-n structures. The J_{sc} was higher in these devices than the majority of p-i-n structures, suggesting lower carrier recombination in the p-n structure.

However, the open circuit voltage (V_{oc}) is significantly reduced for the p-n structure relative to the best p-i-n device. The p-n structures had the same thickness for the CdS and CdTe:As layers and were therefore thinner than the p-i-n devices. Ultra-thin devices typically suffer from pin holes and other defects that can cause shunts which will

reduce the V_{oc}. This is reflected in the large σ for V_{oc} for these p-n structures which may be a result of pinhole defects. The addition of the FeS_x layer may help to reduce these pin holes, which will be reflected in a higher V_{oc}.
Quantum efficiency (QE) was carried out for some of the device samples represented in *Table 1* and the results of the characterisation are shown in *Fig. 4*.

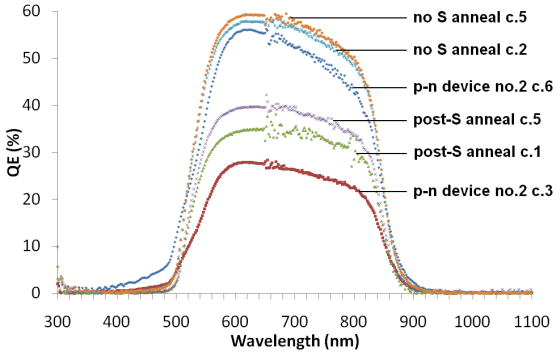

Fig. 4: QE characterisation of different contacts from devices with FeS_x i-layers with and without S annealing, and for a p-n structure without the FeS_x layer.

The p-n structure shows the greatest difference in QE from different contacts on the same device, which demonstrates large lateral inhomogeneity due to its thinner structure having no *i*-layer. The conversion efficiencies were greater for the non-sulphurised p-i-n structure suggesting that the S deficient FeS_x layer was contributing to the device performance. The larger absorption for the sulphurised FeS_x layers observed in T% spectra was not replicated in the QE characterisation of the devices.
The photon conversion cut-off around 850 nm is typical for CdTe–based devices. It was anticipated that the sulphurised p-i-n device structures would show a shift towards longer wavelengths. This was not observed suggesting the majority of electron-hole pairs were generated in the CdTe:As layer. In order to evaluate the FeS_x layer absorption and contribution to device performance in more detail characterisation of devices with thicker FeS_x layers consisting of single phase pyrite and using a thinner CdTe:As p^+ layer is necessary.

Conclusion

Mixed Fe-S phases were obtained by AP-MOCVD which was more suited to low temperature growth. The deposition rate was non-Arrhenius at higher temperatures due to premature thermal decomposition of $FeCO_5$. S annealing of the FeS_x films in a static argon atmosphere showed a transitional phase change to marcasite and pyrite at 400°C.
Devices with p-i-n structures using a non-sulphurised FeS_x layer were observed to have higher η relative to the devices with sulphurised FeS_x layers.
The best non-sulphurised device had similar J_{sc} to the p-n device structures which was significantly higher than the J_{sc} values for the sulphurised devices. This demonstrated a better defined interface at the p-n junction relative to the majority of p-i-n structures. The p-n structures suffered from reduced V_{oc} compared to the best performing non-sulphurised device which is likely due to a thinner structure and larger number of pinholes.
QE showed all devices to have characteristic CdTe absorption suggesting the active layer in the device was the p^+ CdTe:As layer.

References

[1] A. Ennaoui, S. Fiechter, C. Pettenkofer, N. Alonso-Vante, K. Büker, M. Bronold, C. Höpfner, H. Tributsch, *Solar Energy Mat. & Solar Cells* **29** (1993) 289.
[2] D.M. Schleigh, H.S.W. Chang, *J. Crystal Growth* **112** (1991) 737.
[3] B. Meester, L. Reijnen, A. Goossens, J. Schoonman, *Chemical Vapour Deposition* **6** (2000) 121.
[4] C. Höpfner, K. Ellmer, A. Ennaoui, C. Pettenkofer, S. Fiechter, H. Tributsch, *J. Crystal Growth* **151** (1995) 325.
[5] J.R. Ares, A. Pascual, I.J. Ferrer, C. Sánchez, *Thin Solid Films* **480-481** (2005) 477.
[6] Y.Z. Dong, Y.F. Zheng, H. Duan, Y.F. Sun, Y.H. Chen, *Mat. Lett.* **59** (2005) 2398.
[7] A. Ennaoui, S. Fiechter, G. Smestad, H. Tributsch, *Proc. 1st World renewable Energy Congr.*, Reading, UK (1990) 458.
[8] K. Ellmer, H. Tributsch, *Proc. 12th Quantum Solar Energy Conversion Workshop*, Wolkenstein, Südtrirol, Italy (2000).
[9] V. Barrioz, Y. Proskuryakov, E.W. Jones, J. Major, S.J.C. Irvine, K. Durose and D. Lamb, *Mat. Res. Soc. Symp. Proc.* (2007), 1012, Y12-08.
[10] Y.H. Liu, L. Meng, L. Zhang, *Thin Solid Films* **479** (2005) 83.